Resolving single molecule structures with nitrogen-vacancy centers in diamond

Matthias Kost,[1,2] Jianming Cai,[1,2] and Martin B. Plenio[1,2]

[1]*Institut für Theoretische Physik, Albert-Einstein Allee 11, Universität Ulm, 89069 Ulm, Germany*
[2]*Center for Integrated Quantum Science and Technology, Universität Ulm, 89069 Ulm, Germany*

(Dated: 24th July 2014)

We present two-dimensional nuclear magnetic resonance spectroscopy protocols based on nitrogen-vacancy (NV) centers in diamond as efficient quantum sensors of protein structure. Continuous microwave driving fields are used to achieve Hartmann-Hahn resonances between NV spin sensor and proximate nuclei for selective control of nuclear spins and measurement of their polarization. Our protocols take advantage of the strong coupling between the NV sensor and the nuclei, thus facilitating coherence control of nuclear spins and relax the requirement of nuclear spin polarization. We dramatically reduce the experimental effort by employing a singular value thresholding matrix completion algorithm from signal processing to regain the resolution of protein structure based on sub-sampled data from NV based single molecule nuclear magnetic resonance spectroscopy. As an illustration, we demonstrate the power of this approach by identifying the nitrogen-Hydrogen interaction peak in an Alanine spectrum based on merely 5% of the sample data.

arXiv:1407.6262v1 [quant-ph] 23 Jul 2014

INTRODUCTION

Nuclear magnetic resonance spectroscopy (NMR) allows for the structure determination of molecules and proteins and therefore contributes fundamentally to the advancement of the biological sciences. This structural information is obtained by probing the target of investigation by means of multiple radio frequency pulses. The response of the system is then mapped to multi-dimensional spectra which encode the dynamical properties of the system and therefore of the interactions between its constituent nuclear spins [1–3]. This in turn permits the reconstruction of their mutual distances and from this of the entire molecular structure. Due to the minute size of the nuclear magnetic moments compounded by the tiny polarization of these nuclear spins at room temperature, even in very strong magnetic fields, large ensembles (at least 10^{12} molecules) are required in order to extract a measurable signal. Thus NMR is susceptible to inhomogenous broadening and can only deliver ensemble information while the structure and dynamics of individual specimens remain hidden from observation [4–6].

The recent progress in the control of a single electron spin in nitrogen-vacancy (NV) centers in diamond offers a new perspective here as it becomes possible to read out the effect of smallest magnetic fields by means of optically detected magnetic resonance [7–9]. Recent theoretical investigations [10, 11] have suggested that shallowly implanted NV centers [12, 13] in conjunction with dynamical decoupling methods [14–17] should be able to detect and locate individual nuclear spins above the diamond surface. Experimental work achieved the observation of ensembles of nuclear spins outside of diamond [18–20] and recently the detection of small numbers, less than 10, of silicon nuclear spins with a sensitivity that is sufficient to identify even individual nuclear spins [21]. Remarkably, this experiment has also demonstrated a new detection regime in which the NV center (that is the quantum sensor) couples more strongly to the target nuclear spins than these spins are coupling to their neighbours. In consequence, even an unpolarised sample can lead to a signal with full contrast which corresponds to a million-fold improvement of sensitivity over standard NMR [21].

Beyond this remarkable enhancement of the NMR signal, it is important to realize that this new detection regime offers further opportunities beyond the capabilities of standard NMR. In addition to the manipulation and probing of nuclear spins by means of external radio-frequency fields we are now in a position to control the properties of the NV center such as to tailor its response and, crucially, via its strong interaction with nuclei also to obtain an additional handle for the manipulation of the nuclear spins. In this work we take advantage of this potential and demonstrate its usefulness for single molecule spectroscopy.

Despite this progress, the large number of required measurements and the resulting long overall measurement times represent a considerable challenge in single molecule NMR. However, the spectral information that is being obtained in an NMR experiment possesses underlying structure, determined by the Hamiltonian that describes the mutual interactions of the nuclear spins in the molecule, which makes the system sparse in a suitable basis. This fact can be exploited by methods from signal processing such as compressive sensing and matrix completion [22, 23] which are designed to unravel such structures without prior knowledge with the minimal possible number of measurements. Indeed, measuring only a small subset of all accessible data points in time can be shown to allow for the reliable reconstruction of spectral information as it is required in NMR protocols.

In this work we are combining matrix completion and NMR spectroscopy with an NV spin quantum sensor in the strong coupling regime to devise a new regime of

single molecule NMR which has the potential to achieve the elucidation of the structure of individual molecules and proteins. We begin by presenting single molecule two-dimensional (2D)-NMR by means of NV centers in diamond and the efficiency gains that may be achieved by means of matrix completion. We then extend these schemes to the strong coupling regime. For illustration we apply our ideas to a simple bio-molecule, Alanine. We finish the work by discussing the potential for extending these protocols to the membrane proteins whose structure and dynamics are of considerable importance in biology and medicine.

BASIC PRINCIPLES OF 2D NV SPECTROSCOPY

In this section, we will introduce the basic principles of 2D correlation spectroscopy (COSY) that we will realize with an NV quantum sensor, and demonstrate the power of matrix completion in this scenario in the subsequent section. Using a NV quantum sensor that is strongly coupled to external nuclei, it is possible to implement coherent control of the external nuclei, and resolve intermolecular couplings in 2D correlation spectroscopy at the single molecule level. One straightforward way to control the nuclei consists of the use of dynamical nuclear spin polarization via NV centers [26] to strongly polarize a specific set of nuclei, together with radio-frequency pulses as illustrated in Figure 1. We remark that it is possible to avoid the use of radio-frequency pulses by leveraging the strong coupling between the NV spin sensor and the nuclei. The measurement of nuclear spin polarization can then be achieved by the same NV quantum sensor [24]. Neglecting fast oscillating terms, namely under the rotating wave approximation, the dynamics of the NV center and the nuclei in the interaction picture with the microwave drive is governed by the following effective Hamiltonian

$$H_p^{(2)} = \frac{\omega_{nv}}{2}\sigma_x + \omega_f \sum_i \mathbf{s}_i^z + \sum_i g_i^{\parallel}\mathbf{s}_i^z + \sum_i g_i^{\perp}\left(\sigma_x^+ \mathbf{s}_i^- + h.c.\right) \quad (1)$$

where ω_{nv} is the effective Rabi frequency of the field applied to the electronic $|m=-1\rangle \leftrightarrow |m=0\rangle$ transition between of the NV spin in the electronic ground state, and σ_x is the Pauli operator in the corresponding subspace spanned by $\{|m=-1\rangle, |m=0\rangle\}$, σ_x^+ is the raising operator in the eigenbasis of σ_x and $\mathbf{s}_i^-$ represents the nuclear spin lowering operators. For simplicity, we assume the nuclei to be effectively decoupled from each other during the polarization and measurement process. This can be achieved by applying radio frequency fields with a detuning Δ_p from the Larmor frequency of the nuclei and a field strength Ω_p that satisfy $\Omega_p = \sqrt{2}\Delta_p$, which leads to an effective nuclei energy scale $\omega_f = \sqrt{\Delta_p^2 + \Omega_p^2}$ [24]. If the refined effective Hartmann-Hahn condition

$$\Omega_{nv} = (\gamma_N B - \Delta_p) + \omega_f, \quad (2)$$

is fulfilled, electron-nuclear spin-flip-flop processes lead to polarization exchange between the NV center spin and the nuclei and result in the efficient polarization of the nuclear spins. We can infer the average polarization of the nuclei from the measurement signal of the NV center spin by [24]

$$\Delta_P = P_-^+ - P_+^- = 2\tau^2 \sum_i (g_i^{\perp})^2 \langle \mathbf{s}_i^z \rangle \quad (3)$$

where $P_\mu^\nu(\mu, \nu = \pm)$ is the population of the NV center in state $|\nu\rangle$ after being initialized in state $|\mu\rangle$ and a free evolution determined by eq. (1) for a period of time τ. The nuclear polarization in x and y direction can be measured similarly by applying an additional pulse to rotate the nuclear spins before performing the NV measurements [24].

In our 2D spectroscopy protocol, the measurement results of the final nuclear spin polarizations following free evolution times t_1 and t_2 can be arranged in a polarization matrix in the time domain, S_t for $t = (t_1, t_2)$, the Fourier coefficients of which yield the 2D spectra. The resulting diagonal peaks refer to the Larmor frequencies

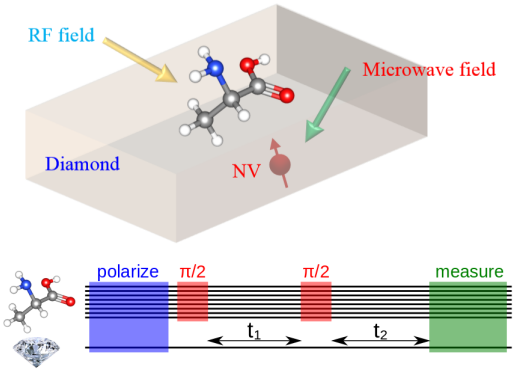

Figure 1: Two-dimensional correlation spectroscopy (COSY) pulse sequence. The nuclei (upper row of horizontal lines) are initially polarized by a NV spin sensor (blue box) and prepared into a coherent superposition by the subsequent application of a radio-frequency $\pi/2$-pulse (red box) on the nuclei only. The nuclei then undergo a free evolution for time t_1 followed by a second radio-frequency $\pi/2$-pulse (red box). After a further free evolution time t_2, the polarization of nuclear spins is selectively measured by a NV spin sensor (green box). During the free evolution times, the interaction between the NV center electron spin and the nuclei is eliminated by transferring the NV spin to the $m_s = 0$ ground state.

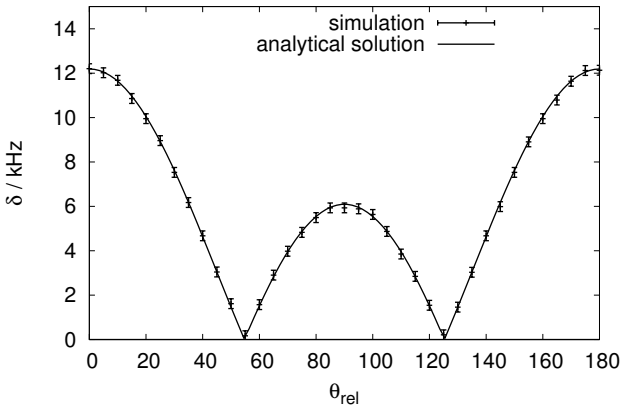

Figure 2: The angular dependence of the energy splitting due to dipole-dipole interaction in the basic example of two Hydrogen atoms. The error bars are included to account for the possible read-out error given by the resolution of the discrete Fourier transform, which is bounded by the inverse of the physical experiment time. The solid line refers to the analytical solution based on the used geometric parameters.

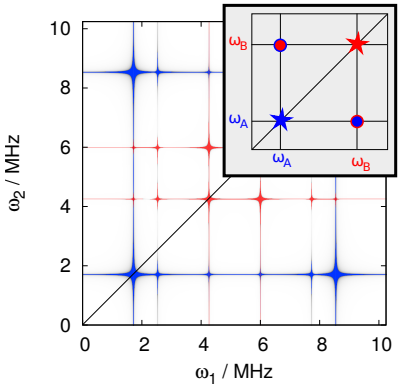

Figure 3: The spectra of Hydrogen (red) and Phosphorus (blue) for a simple 2-atom computation. Inlet: Symbolic representation of the spectrum of atom A (red) and B (blue) respectively. Both spectra show a diagonal peak (star) that refers to the Larmor frequency of the corresponding atom and an off-diagonal polarization exchange peak (filled circles) located at (ω_A, ω_B) with $\omega_A \neq \omega_B$. The height of off-diagonal peaks indicates the coupling strength of the two atoms. Further peaks may arise at positions that correspond to certain integer linear combinations of the Larmor frequencies for multi-particle systems. Although the corresponding frequencies may exceed the maximally resolvable frequency given by the sampling theorem, aliasing leads to projections into the resolvable range.

of individual nuclear spins, and the off-diagonal peaks indicate polarization exchange between pairs of nuclei in the target molecule.

We demonstrate the basic working principle of our protocol at the hand of the simple example of two Hydrogen atoms at a distance of $\sim 1 - 2\mathring{A}$, which is the typical distance in proteins. The splitting due to their dipolar interaction is plotted for different magnetic field orientations to validate the dependency of the splitting on the magnetic field orientation

$$\delta_{dd} = \frac{\mu_0}{4\pi}\frac{\hbar\gamma_a\gamma_b}{r^3}(3\cos^2\theta - 1) \tag{4}$$

where r is the distance between two nuclei, $\cos\theta = \hat{b}\cdot\hat{r}$ with $\hat{b}$ and $\hat{r}$ the unit direction vector of the magnetic field and the vector that connects two nuclei respectively and γ_a, γ_b are the nuclear gamma factors, see Figure 2. In our numerical simulation, we assume an applied magnetic field of 1000G during the nuclear spin free evolution time, to resolve the dipole-dipole energy splitting of a few kHz, the physical simulation times are set to a few milliseconds. In spherical coordinates with the z axis aligned with the connection vector $\vec{r}$, the splitting is degenerate with respect to rotations about the z-axis, only the projection $\cos\theta$ is relevant for the absolute energy splitting. Varying the magnetic field orientation (with three possible directions), one can extract the relative orientation of pairs of nuclei in the sample by fitting Eq. (4) into the splitting of matching pairs. To obtain the values of r and θ, two independent magnetic field directions are sufficient.

Furthermore, it is also possible to identify the polarization exchange peak from the above NV based 2D spectroscopy. As an example, we simulate the 2D spectrum of a functional group that consists of a Hydrogen and a Phosphorus atom with an intranuclear distance of $\sim 2\ \mathring{A}$ under the application of a magnetic field of 1000G. Under these conditions the difference between the Larmor frequencies of Hydrogen and Phosphorus is sufficiently large to fulfill a selective Hartmann-Hahn condition [10], that is we can tune the microwave Rabi frequency to match separately the resonance condition with Hydrogen and Phosphorus. As a result, the NV spin only effectively interacts with one species of nuclei.

Our numerical simulations suggest that a few hundred microseconds of evolution time is sufficient to resolve the various peaks in the 2D spectrum associated with this system. The spectral representation of the corresponding NV signal will be referred to as the Hydrogen spectrum, and as the Nitrogen spectrum respectively. The spectral peaks arising from the dipolar interaction between nuclear spins appear off-diagonal at the coordinates determined by a pair of Larmor frequencies of Hydrogen and Nitrogen, as shown in Figure 3. Therefore, we can gain full information about the hyperfine interaction between two nuclei, and extract their structure information accordingly.

MATRIX COMPLETION FOR AN NV-BASED 2D NMR

For larger molecules, the application of NV-based 2D-NMR suffers from a rapidly increasing experiment effort as a function of the number of nuclei in the target molecule. In this section, we explain that the experimental overhead of NV-based 2D spectroscopy can be reduced significantly by exploiting the technique of matrix completion [22, 23] which exploits two specific aspects of NV-based 2D spectroscopy. First, 2D-spectra generally possess structure which expresses itself in sparseness in a certain basis and, secondly, while the relevant information is represented in Fourier space, the experimental data are taken in time. We will begin by clarifying why these two aspects are important and how they are going to be being used.

For a given matrix A we denote with σ_i its descendingly ordered singular values, that is the diagonal entries of the matrix D in $A = U\Sigma V^\dagger$ where U and V are unitaries. If these singular values are close to zero for indices $i > r$, one obtains a high fidelity approximation $\tilde{A}$ with rank r for the matrix A by

$$\tilde{A} = U\tilde{\Sigma}V^\dagger \tag{5}$$

where $\tilde{\Sigma}$ is a low rank version of Σ, as defined by

$$\tilde{\Sigma}_{ij} = \begin{cases} \sigma_i, & i = j \leq r \\ 0, & \text{else} \end{cases} \tag{6}$$

The idea of matrix completion is to reconstruct the matrix A by finding a low rank approximation $\tilde{A}$ based on the knowledge of a few entries from a random sample set $\{(i,j)\} = \Omega$ such that $\left\| \mathcal{P}_\Omega \times (A - \tilde{A}) \right\| < \epsilon$, where $\mathcal{P}_\Omega$ is a boolean matrix that indicates whether (i,j) is in Ω or not and $\times$ means elementwise multiplication.

It is important to note that generally the basis in which one takes the random samples will affect the reconstruction efficiency. Indeed, sampling a matrix with just one nonzero entry, i.e. a very sparse matrix, will tend to yield only zeros upon random sampling of the matrix entries and hence any reconstruction algorithm must conclude that the matrix is in fact zero. This situation differs considerably when we take the discrete Fourier transform of this matrix and sample the result. Now sampling even a small number of entries will yield useful information about the structure of the matrix and indeed it becomes possible then to reconstruct this Fourier transformed matrix (and hence also the original) from a small number of sampled entries (for a $n \times n$ matrix the number of required samples scales as $rn \ln n$ where r is the singular value rank of the data matrix). Indeed, for a matrix that is sparse in some basis $\{|e_i\rangle\}$ (i.e. most of its entries vanish or are negligible) it is in this sense optimal to sample the matrix in the Fourier transformed basis $\{\mathcal{F}|e_i\rangle\}$ (see e.g. [25] for mathematical proofs that support this observation).

It is essential that the data matrices that one obtains from NV-based 2D-NMR tend to be or approximately sparse as their entries are concentrated on the diagonal and around the off-diagonal positions that indicate coupling between those diagonal elements. From these arguments and observations it becomes transparent that matrix completion is ideally suited to support NV-based NMR spectroscopy as the desired information is represented in frequency while the data are taken in time, that is we sample the desired information in a basis that is Fourier transformed with respect to the information basis. We will make use of this fact in the remainder of this section.

As a demonstration of the efficiency of matrix completion algorithms in our NV-based 2D spectroscopy, we simulate a NMR spectrum of an Alanine molecule based on an NV-based COSY NMR simulation as described in the above section. We assume a shallowly implanted NV center located in a distance of 2nm to the surface [21] to measure the polarization of the Hydrogen and Nitrogen atoms by matching the resonance condition for the two species respectively so that we can obtain the corresponding magnetic resonance spectra. Alanine is one of the smallest amino acids with chemical composition HOCCH(NH)CH, so for NMR there are 7 Hydrogen atoms and a single Nitrogen atom. The molecule has a total size of about 0.45nm and is illustrated in Figure 4 (inset). We assume a magnetic field of 1000G, and the intensities of the microwave and radio frequency fields are tuned to be $\Omega_{nv} = \omega_f = 200$kHz, see Eq. (1-2), to effectively decouple nuclear spin-spin interaction during the selective measurement process. We simulate a subset of the entries S_t corresponding randomly chosen $t = (t_1, t_2)$, which are those data that would be measured in real experiments. The completion algorithm will reconstruct the 1024×1024 time domain matrix S_t out of the subsampled entries (sampling rate approximately 5%). We will see that in the frequency domain, the Nitrogen-Hydrogen polarization exchange peak can then be identified from the reconstructed matrix.

As a comparison, we plot in Figure 4(a) the spectrum obtained from the complete set of measurements, namely based on a 100% data sample. Figure 4(b) shows the same as the inlet in Figure 4(a), for different sample rates. It can be seen that we are able to identify the polarization exchange peak of Nitrogen in the Hydrogen signal even with only 5% data sample. To characterize how well the procedure works, we define the Frobenius error (with the weighting matrix W to allow us to concentrate on specific parts of the spectrum if desired) of the completed matrix C from our procedure with respect to the exact

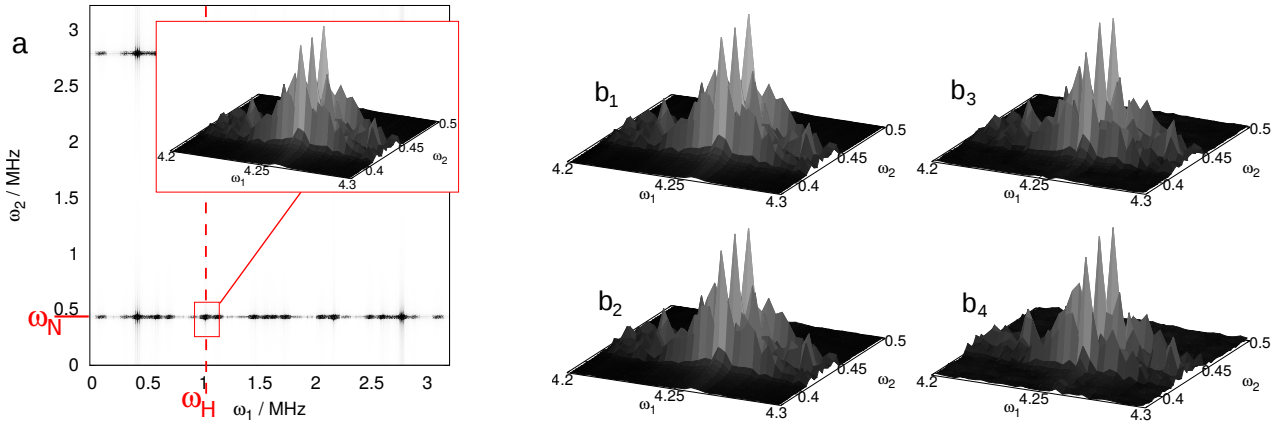

Figure 4: The magnetic resonance spectra of an Alanine molecule based on an NV-based COSY NMR and matrix completion. **(a)** The spectral representation of the NV signal when the Hartmann-Hahn resonance condition is satisfied for Nitrogen. The Hydrogen Larmor peak shows up on the diagonal at 4.24 MHz (this peak is located at 1 MHz due to aliasing). The dashed line shows the Larmor frequency of Nitrogen at 0.43 MHz. The off-diagonal peak at $(0.43, 4.24)$ MHz represents polarization exchange between Hydrogen and Nitrogen atoms. The inlet shows the local environment of that peak as a 3D surface plot. **(b)** Comparison of the local environment of the peaks from the inlet in **(a)** for different sample rates. b_1) full data. b_2) 20% data sample. b_3) 10% data sample. b_4) 5% data sample.

underlying matrix R as

$$\epsilon_F = \frac{\sum_{ij} w_{ij}^2 (\alpha C_{ij} - R_{ij})^2}{\sum_{ij} w_{ij}^2 R_{ij}^2} = \frac{\|W \times (\alpha C - R)\|_F}{\|W \times (R)\|_F}, \quad (7)$$

where $\|\cdot\|_F$ denotes the Frobenius norm and α is a scalar which was introduced to compensate for a rescaling due to the completion algorithm. The weighting option was introduced in order to be able to assess the error for specific parts of the spectrum that carry the physically relevant information such as diagonal and cross peaks. Errors of values close to zero that suffer from noise and distortion receive less weight due to the weighting option, as such fluctuations are expected to show up especially in those small singular values that are neglected in the low rank approximation. The relative error of the completed time domain data does not appear to influence the peak positions, which are relevant for the spectra. For the spectral domain, the weighted error (concentrating on the diagonal and off-diagonal peaks only) is very small in comparison to the non-weighted error, which allows us to conclude that these peaks are well reconstructed and a significant part of the noise mainly appears in smaller matrix elements. Hence we expect a remarkable time saving due to sub-sampling of both experimental and simulated data for sufficiently large matrices.

EXPLOITING THE STRONG COUPLING REGIME

One important feature of an NV center sensor is that it can be located very close to the diamond surface, and thus to the target molecule. Recent experiments have shown that NV centers as shallow as 2nm can still have sufficiently good properties to be an effective sensor [20, 21]. Under these circumstances, the coupling between the NV center spin can exceed the inter-nuclear couplings within the molecule. An NV quantum sensor in such a strong coupling regime provides stronger signals, which scale as a linear function (instead of the square root) of the number of nuclei. More importantly, operating in this regime, it is not necessary to polarize nuclear spins, while still retaining a full signal contrast due to the quantum nature of the interaction between the NV center spin and the nuclei. Moreover, we can make use of the strong coupling for the coherent control of both nuclear spins (by means of radio-frequency fields or via the interaction with the NV center) and of the NV center spin (microwave frequency fields) thus allowing for more complex pulse sequences for the simultaneous control of sensor and target.

As an illustrative example, we construct a novel NV-based 2D-spectroscopy scheme by exploiting the strong interaction of nuclei in a target molecule with an NV center spin, see Figure 5(a). Here we selectively trigger the NV-nuclear spin interaction to generate entanglement between the NV center and the nuclear spins interspersed with free evolution times t_1 and t_2 which in turn allow for an accumulation of the effect of the nuclear Hamiltonian that can subsequently be measured via the NV center. While this scheme appears similar to the well-known COSY sequence it differs from it due to the entanglement that is created between NV center and nuclear spin which in turn allows us to generate the same spectral information as in the case of COSY with fully polarized nuclear spins but now without the need for nuclear spin polarization. Although the actual detection protocol is

quite different, this scheme shares sufficient parallels to the COSY scheme from figure 1 to transfer the interpretation of peak positions from the original COSY scheme.

For definitness, we describe the pulse sequence in detail together with the relevant Hamiltonians (see also fig. 5, top):

- *Initialization*: the NV center is initialized in a polarized state, while the nuclear spins remain unpolarized (blue bar).
- *NV-nuclear interaction*: the NV center interacts with the nuclei for a time τ (red bar). In this step the NV center becomes entangled with the nuclear spins. The dynamics is governed by the Hamiltonian eq. (1).
- *Free evolution period 1*: the interaction of the NV center with the nuclei is switched off by transfer of the NV center to the $m = 0$ state and if necessary the quantum information may be transferred to the nuclear spin degree of freedom of the NV center and the nuclear spins precess freely for a time t_1 during which the dynamics is governed by the Hamiltonian

$$H_B = \sum_i \gamma_i \mathbf{B} \cdot \mathbf{s}_i + \sum_{i \neq j} g_{ij} \left(\mathbf{s}_i \cdot \mathbf{s}_j - 3(\hat{\mathbf{r}}_{ij} \cdot \mathbf{s_i})(\hat{\mathbf{r}}_{\mathbf{ij}} \cdot \mathbf{s_j}) \right) \quad (8)$$

- *NV-nuclei interaction*: The NV center again interacts with the nuclei with the same Hamiltonian eq. (1). The additional entanglement depends on the system state after the previous free evolution time t_1.
- *Free evolution period 2*: the interaction with the NV center is switched off and the nuclear spins precesses freely for a time t_2 under the same Hamiltonian as in the free evolution period 1.
- *NV-nuclear interaction*: A third interaction employing the same dynamics as in the previous two NV-nuclear interaction periods prepares the final measurement.
- *Measurement*: Finally, we perform a projective measurement on the initial state of the NV center spin (green bar).

As illustration of the above 2D NMR protocol with a strongly coupled NV center at a depth of 2 nm we consider Alanine in a magnetic field of 100G. The simulated magnetic resonance spectra is plotted in Figure 5(b), from which one can clearly identify the polarization exchange peak between the Hydrogen and Nitrogen. Assuming that the nuclei are initially not polarized, we have also verified that they will remain nearly unpolarized across the entire pulse sequence, that is we observe

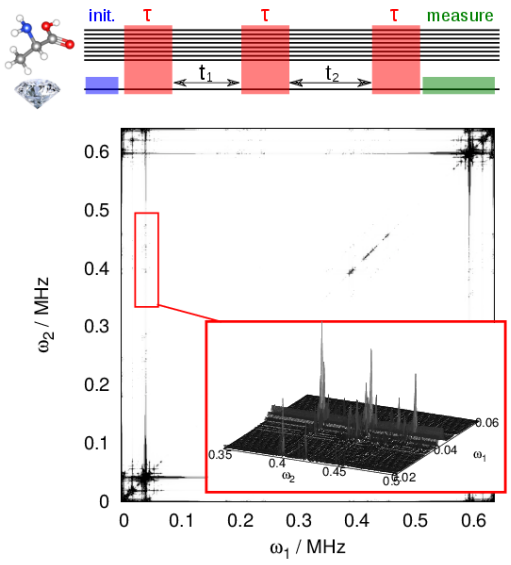

Figure 5: 2D NMR spectroscopy pulse sequence with an NV sensor in the strong coupling regime. **top:** Strong coupling 2D NMR pulse sequence. The nuclei are initially unpolarized, only the NV center is initialized in a $m = \pm 1$ state. The final measurement is a projection of the NV center onto its initial state. During the free evolution times $t_{1,2}$, the NV-nuclear interaction is effectively eliminated, while it is switched on during the periods τ. **bottom:** Resulting spectrum for an NV center tuned on resonance to the Nitrogen transition at a magnetic field of 100G aligned to the NV axis. $t_{1,2}$ was varied up to 1.6ms, while the time τ has to be much larger to have sufficient contrast in the measurement signal. Due to the long simulation times, the hyperfine coupling is resolved.

NMR signals without relying on any nuclear polarization, which represents a distinct feature as compared with conventional NMR techniques.

CONCLUSIONS AND DISCUSSIONS

We have demonstrated the feasibility of two-dimensional nuclear magnetic resonance spectroscopy protocols based on nitrogen-vacancy centers in diamond as sensitive probes of protein structure. In particular, we show that an NV sensor in the strong coupling regime offers new opportunities that can reduce the experimental requirements both by relaxing the need for nuclear spin polarization while retaining a significant signal and by reducing significantly the number of measurements required to recover the 2D spectrum. The latter goal is achieved by matrix completion, a method from signal processing. We find in our numerical simulation, that the computational overhead for the completion process is negligible in comparison to the effort of computing the full spectrum via simulation [27] or the time required to obtain the full spectrum in experiment.

ACKNOWLEDGEMENTS

We thank Fedor Jelezko and Boris Naydenov for discussion concerning experimental issues. This work was supported by an Alexander von Humboldt professorship, the DFG SFB TR/21, the EU Integrating Projects SIQS and DIADEMS, the EU STREP EQUAM, and the ERC Synergy grant BioQ.

[1] J. Jeener, Lecture Notes of the Ampere School in Basko Polje, Yugoslavia 1971 reprinted in NMR and More in Honour of Anatole Abragam, Eds. M. Goldman and M. Porneuf, pp. 1 - 379, Les editions de physique (1994).

[2] W. P. Aue, E. Bartholdi and R. R. Ernst, J. Chem. Phys. 64, 2229 (1976).

[3] R.R. Ernst, G. Bodenhausen and A. Wokaun. Principles of Nuclear Magnetic Resonance in One and Two Dimensions. Oxford University Press, Oxford (1989).

[4] E. Barkai, Y. Jung and R. Silbey, Ann. Rev. Phys. Chem. **55**, 457 (2004).

[5] A. A. Deniz, S. Mukhopadhyay and E. A. Lemke, J. R. Soc. Interface **5**, 15 (2008).

[6] S. J. Lord, H. D. Lee and W. E. Moerner, Anal. Chem. **82**, 2192 (2010).

[7] J. R. Maze, P. L. Stanwix, J. S. Hodges, S. Hong, J. M. Taylor, P. Cappellaro, L. Jiang, M. V. Gurudev Dutt, E. Togan, A. S. Zibrov, A. Yacoby, R. L. Walsworth and M. D. Lukin Nature **455**, 644 - 647 (2008).

[8] G. Balasubramanian, I. Y. Chan, R. Kolesov, M. Al-Hmoud, J. Tisler, C. Shin, C. Kim, A. Wojcik, P. R. Hemmer, A. Krueger, T. Hanke, A. Leitenstorfer, R. Bratschitsch, F. Jelezko and J. Wrachtrup, Nature **455**, 648 - 651 (2008).

[9] C. L. Degen, Appl. Phys. Lett. **92**, 243111 (2008)

[10] J.-M. Cai, F. Jelezko, M. B. Plenio, and A. Retzker, New Journal of Physics **15**, 013020 (2013).

[11] Viktor S. Perunicic, Liam T. Hall, David A. Simpson, Charles D. Hill, Lloyd C. L. Hollenberg, arXiv:1307.8220.

[12] B. K. Ofori-Okai, S. Pezzagna, K. Chang, M. Loretz, R. Schirhagl, Y. Tao, B. A. Moores, K. Groot-Berning, J. Meijer, C. L. Degen, Phys. Rev. B **86**, 081406 (2012).

[13] T. Staudacher, F. Ziem, L. Häussler, R. Stöhr, S. Steinert, F. Reinhard, J. Scharpf, A. Denisenko, A., Wrachtrup, J. Appl. Phys. Lett. **101**, 212401 (2012).

[14] B. Naydenov, F. Dolde, L.T. Hall, C. Shin, H. Fedder, L.C.L. Hollenberg, F. Jelezko and J. Wrachtrup, Phys. Rev. B **83**, 081201 (2011).

[15] J.-M. Cai, F. Jelezko, N. Katz, A. Retzker and M. B. Plenio, New J. Phys. 14, 093030 (2012).

[16] J.-M. Cai, B. Naydenov, R. Pfeiffer, L. McGuinness, K.D. Jahnke, F. Jelezko, M. B. Plenio and A. Retzker, New J. Phys. 14, 113023 (2012).

[17] Z.-Y. Wang, J.-M. Cai, A. Retzker and M. B. Plenio. arXiv:1404.1190

[18] T. Staudacher, F. Shi, S. Pezzagna, J. Meijer, J. Du, C. A. Meriles, F. Reinhard, and J. Wrachtrup, Science **339**, 561 (2013).

[19] H. J. Mamin, M. Kim, M. H. Sherwood, C. T. Rettner, K. Ohno, D. D. Awschalom, and D. Rugar, Science **339**, 553 (2013).

[20] S. J. DeVience, L. M. Pham, I. Lovchinsky, A. O. Sushkov, N. Bar-Gill, C. Belthangady, F. Casola, M. Corbett, H. Zhang, M. Lukin, H. Park, A. Yacoby, R. L. Walsworth, arXiv:1406.3365.

[21] C. Müller, X. Kong, J.-M. Cai, K. Melentijevic, A. Stacey, M. Markham, J. Isoya, S. Pezzagna, J. Meijer, J.-F. Du, M. B. Plenio, B. Naydenov, L. P. McGuinness, F. Jelezko, To appear in Nat. Comm. (2014).

[22] E.J. Candes and M. B. Wakin, IEEE Signal Processing Magazine **25**, 21-30 (2008).

[23] J.-F. Cai, E. J. Candes, and Z. Shen, SIAM J. on Optimization **20**, 1956 (2010).

[24] J.-M. Cai, A. Retzker, F. Jelezko, and M. B. Plenio, Nature Physics, **9**, 168-173 (2013).

[25] D. Gross, IEEE Trans. Inf. Theo. **57**, 1548 - 1566 (2011)

[26] P. London, J. Scheuer, J.-M. Cai, I. Schwarz, A. Retzker, M. B. Plenio, M. Katagiri, T. Teraji, S. Koizumi, J. Isoya,R. Fischer, L. P. McGuinness, B. Naydenov, F. Jelezko, Phys. Rev. Lett. **111**, 067601 (2013).

[27] J. Almeida, J. Prior and M. B. Plenio, J. Phys. Chem. Lett., **3**, 2692-2696 (2012).